

1-1-1999

## On the experimental search for photon mixing

VSEVOLOD POPOV

Follow this and additional works at: <https://journals.tubitak.gov.tr/physics>



Part of the [Physics Commons](#)

---

### Recommended Citation

POPOV, VSEVOLOD (1999) "On the experimental search for photon mixing," *Turkish Journal of Physics*: Vol. 23: No. 5, Article 17. Available at: <https://journals.tubitak.gov.tr/physics/vol23/iss5/17>

This Article is brought to you for free and open access by TÜBİTAK Academic Journals. It has been accepted for inclusion in Turkish Journal of Physics by an authorized editor of TÜBİTAK Academic Journals. For more information, please contact [academic.publications@tubitak.gov.tr](mailto:academic.publications@tubitak.gov.tr).

# On the experimental search for photon mixing

Vsevolod POPOV\*

*Institute of Nuclear Research of Russian Academy of Sciences  
7a, 60 October Anniv. Prosp., Moscow 117312 RUSSIA*

Received 02.02.1999

## Abstract

The experimental searches for photon mixing in the Okun model [1] are discussed.

## 1. Introduction

“Paraphotons” were first introduced in [1] within a framework of electrodynamics with two massive photons. In fact, this theory presents itself a natural development investigations involving a single massive photon (cf., for example, reviews [2,3], the best *direct* limit on a photon mass [4] or recent works [5]). The Lagrangian proposed by [1] has the form

$$\mathcal{L} = -F_{1\mu\nu}^2 - F_{2\mu\nu}^2 + m_1^2 A_{1\mu}^2 + m_2^2 A_{2\mu}^2 + j_\mu (e_1 A_{1\mu} + e_2 A_{2\mu}), \quad (1)$$

with fields  $A_1$  and  $A_2$  of masses  $m_1$  and  $m_2$  and coupling constants  $e_1$  and  $e_2$ , respectively. The ordinary photon is replaced in this formalism by the interacting state

$$\gamma = (e_1 A_1 + e_2 A_2)/e \quad , \quad e^2 = e_1^2 + e_2^2.$$

There exists also a non-interacting (sterile) state

$$\gamma_s = (-e_2 A_1 + e_1 A_2)/e \quad ,$$

that we will call (after [1]) the paraphoton. It is convenient to use a mixing angle  $\theta$  :  $\sin \theta = e_2/e$ , so that the mixing between  $(\gamma, \gamma_s)$  and  $(\gamma_1, \gamma_2)$  (the latter stands for the fields  $A_1, A_2$ ) could be written as

$$\begin{pmatrix} \gamma \\ \gamma_s \end{pmatrix} = \mathbf{M} \begin{pmatrix} \gamma_1 \\ \gamma_2 \end{pmatrix} \quad , \quad \mathbf{M} = \begin{pmatrix} \cos \theta & \sin \theta \\ -\sin \theta & \cos \theta \end{pmatrix}. \quad (2)$$

---

\*e-mail: vpopov@vxjinr.jinr.ru

The observable effects that follow from this model were described in [1]; some modifications were made in [6]. Most of the effects could be divided into the “static” cases (deviations from the Coulomb law and the equations of magnetostatics) and the photon oscillations arising due to the mass difference. We will concentrate here on the experiments exploring the oscillations and mention briefly only the static effects relevant for our field of mixing parameters.

**2. Static limits**

The Coulomb potential in this model takes the form [1] :

$$U(r) = \frac{e^2}{4\pi r} (\cos^2 \theta e^{-m_1 r} + \sin^2 \theta e^{-m_2 r}) \tag{3}$$

If we choose  $\gamma_1$  for the principal component of our interacting  $\gamma$  by taking  $0 \leq \theta \leq \pi/4$  then it immediately follows from (3) that  $m_1$  is strongly constrained. The maximal value allowed is about the same as the limit put on the photon mass in the model of a single massive photon [1-4]. The strongest limits are obtained from the observations of large-scale magnetic fields (for example, of Jupiter [4] or galactic ones [1]), as for the static magnetic fields one will also have the terms of the order of  $m_1 r$ . For the rest of the paper we take  $m_2 \gg m_1 \approx 0$ , and  $m \equiv m_2$  and  $\sin \theta$  will be the only mixing parameters.

On Figure. 1 we plot existing and reachable future limits (or the regions of the possible discovery. . .) for mixing parameters in the  $\sin^2 2\theta - m$  plane. The excluded regions lie above the corresponding curves. For units of mass, we use both  $eV$  and  $cm^{-1} \approx 2 \cdot 10^{-5} eV$  with  $\hbar = c = 1$ .

The curve marked “Coulomb” stands for the combined result of experiments [7] that investigated the validity of Coulomb law by measuring the electric field between the concentric spheres (with the radii of the order of 10 --100 cm). In [8] are results comparing the Rydberg constants for the atomic transitions between the high- and low-lying atomic levels, thus being most sensitive to the atomic scale of  $10^{-7} \dots 10^{-8} cm$ . It is not easy to devise a “static” experiment covering a large gap between the two; in this region oscillations work better.

**3. Oscillations formalism**

We consider here “aromatic” states  $\gamma$  and  $\gamma_s$  ( eigenstates of interactions) and “mas-sive” states  $\gamma_1$  and  $\gamma_2$  (eigenstates of the propagation in vacuum), with the mixing of (2) between them.

In a general case, photon propagation could be described by the Shroedinger-like equation :

$$i \frac{d}{dt} \begin{pmatrix} \gamma \\ \gamma_s \end{pmatrix} = \begin{pmatrix} V_{\gamma\gamma} & V_{\gamma_s} \\ V_{\gamma_s} & V_{s_s} \end{pmatrix} \begin{pmatrix} \gamma \\ \gamma_s \end{pmatrix} \tag{4}$$

with  $V_{\gamma\gamma}$  and  $V_{s_s}$  – amplitudes of the transitions  $\gamma \rightarrow \gamma$  and  $\gamma_s \rightarrow \gamma_s$  and  $V_{\gamma_s}$  – as the mixing amplitude. Solving it for the constant and real amplitudes with the boundary

conditions  $\gamma(t=0) = 1, \gamma_s(t=0) = 0$ , we get the probability of the transition  $\gamma \rightarrow \gamma_s$ <sup>1</sup>:

$$P_{\gamma \leftrightarrow \gamma_s} = \frac{4V_{\gamma_s}^2}{(V_{\gamma\gamma} - V_{ss})^2 + 4V_{\gamma_s}^2} \sin^2 \left( \frac{t}{2} \sqrt{(V_{\gamma\gamma} - V_{ss})^2 + 4V_{\gamma_s}^2} \right). \quad (5)$$

In vacuum, (4) and (5) will take the well known forms for neutrino oscillations [9]:

$$i \frac{d}{dx} \begin{pmatrix} \gamma \\ \gamma_s \end{pmatrix} = \begin{pmatrix} -\frac{m^2}{2\omega} \cos 2\theta & \frac{m^2}{4\omega} \sin 2\theta \\ \frac{m^2}{4\omega} \sin 2\theta & 0 \end{pmatrix}, \quad (6)$$

$$P_{vac} = \sin^2 2\theta \sin^2 \left( \pi \frac{L}{L_\gamma} \right), \quad L_\gamma = \frac{4\pi\omega}{m^2} = 1.57 \cdot 10^6 \text{ cm} \left( \frac{\omega}{2.5 \text{ eV}} \right) \left( \frac{1 \text{ cm}^{-1}}{m} \right)^2, \quad (7)$$

for photon of energy  $\omega$  after travelling a path  $L$ . It is valid for the ultra-relativistic case ( $\omega \gg m$ , so  $t \approx L$ ) and the uncertainty in photon energy  $\Delta\omega \gg m^2/2\omega$ . The latter effectively defines the right edge of all the “non-static” curves in Figure 1 and can be taken as an approximation only; more realistic treatment requires a wave-packet formalism. We suppose that it would produce the results close to ours. The same stands for the situations when  $x \gg L_\gamma$  and we have a large number of the oscillation periods. In this case we take an average 0.5 for the oscillatory  $\sin^2$  of (7). In fact, oscillations die out over long distances because of wave packets separation; but our averaging should give plausible results for reasonable wave packets shapes.

In the medium one should take into account photon interactions. First, there are “incoherent” processes, such as absorption, refraction or reflection: the paraphoton does not processes suffer from these. It is possible to keep completely the above formalism and add to  $V_{\gamma\gamma}$  the corresponding *imaginary* amplitudes. We choose to consider the oscillations at the free path of a photon between two interactions, thus keeping the amplitudes real. Second, the “coherent” contribution by the “optical density” of the medium; it could be described by adding the corresponding *real* term to the  $V_{\gamma\gamma}$ . Typical examples are an “ordinary” refractive medium (for the visible light) and a plasma (in plasma frequency approximation); for them the oscillation probabilities will look as follows:

$$P_{\gamma \leftrightarrow \gamma_s} = \frac{\sin^2 2\theta}{(\cos 2\theta + R)^2 + \sin^2 2\theta} \sin^2 \left[ \frac{\pi L}{L_\gamma} \sqrt{(\cos 2\theta + R)^2 + \sin^2 2\theta} \right], \quad (8)$$

$$R = \begin{cases} 4.7 \cdot 10^6 \left( \frac{\omega}{2.5 \text{ eV}} \right)^2 \left( \frac{1 \text{ cm}^{-1}}{m} \right)^2 \left( \frac{n-1}{3 \cdot 10^{-4}} \right) & \text{in the air;} \\ -2.3 \cdot 10^{12} \left( \frac{\omega_{pl}}{30 \text{ eV}} \right)^2 \left( \frac{1 \text{ cm}^{-1}}{m} \right)^2 & \text{in the plasma.} \end{cases} \quad (9)$$

Here,  $n$  denotes the refraction index and  $w_{pl}$  the plasma frequency. We use here the typical values for the cases that we will consider. Note negative sign for  $R$  in the plasma

<sup>1</sup>The same as for the transition  $\gamma_s \rightarrow \gamma$  in a case of  $\gamma(t=0) = 0, \gamma_s(t=0) = 1$ .

case; it makes a resonant solution [10] possible. But generally for the low masses a medium suppresses the amplitude of the oscillations and shortens the period.

#### 4. Solar paraphotons

For our purposes, the Sun is a huge cauldron filled with the photons. Each of them has a certain probability to convert to a paraphoton which would escape freely from the Sun (unless  $\sin^2 2\theta$  is too large [6]) resulting in energy loss. As the solar models [11,12] are considered to be precise enough, one may assume that the illegal loss should not exceed the measured luminosity of the Sun. This constraint on the mixing parameters was discussed in [1] and, in more detail, in [6]. The “Sun” curve in Figure 1 presents a recalculation of the result from [6] using the data from [12] that covers more completely the outer layers of the Sun. This is important for low paraphoton masses. Other changes were made for the solar opacities that determine a free path of the photon in the Sun ( $\equiv$  oscillation base). These were taken from [13] instead of using an approximation as in [6]. We do not consider possible resonant oscillations in the solar plasma.

For the calculations, the Sun was divided into 30 spherical layers and the physical parameters were taken as constant within each one; this caused the solar curves in the plot to be non-smooth. The results obtained for the different mixing parameters were used for evaluations of energy loss, both total and specific to the spectral regions covered by the experiments.

#### 5. Experiments

All experiments described in this section are essentially of the double oscillations type, or “shining light through the wall”: the photons emitted by a certain source acquire at their propagation an admixture of paraphotons by the oscillations. All photons are blocked except the sterile component which penetrates a block and then oscillates again to the photons which are detected.

##### 5.1. Laser shining through the wall [14]

This experiment employed a laser beam directed onto the block from the distance of 440 cm; at the same distance beyond the block a sensitive photodetector counted the photons. A rotary chopper controlled a “light on/off” state and special precautions were taken to ensure the equality of the times spent in the two states. With effective laser power of 300 W and noise level of 0.6 Hz data was obtained over 60,000 seconds of running time and produced a counting rate  $\Delta(ON - OFF) = 0.004 \pm 0.002 \text{ Hz}$  thus, providing a  $2\sigma$  signal in favour of “photon regeneration”. A corresponding constraint at the level of  $3\sigma$  is plotted with asterisks and marked “laser” at Fig. 1.

##### 5.2. Hunting for the solar paraphotons

As stated in Sec.4, the Sun presents a ready source of paraphotons due to oscillations within its volume. Any device “observing” the Sun through the *opaque* window would

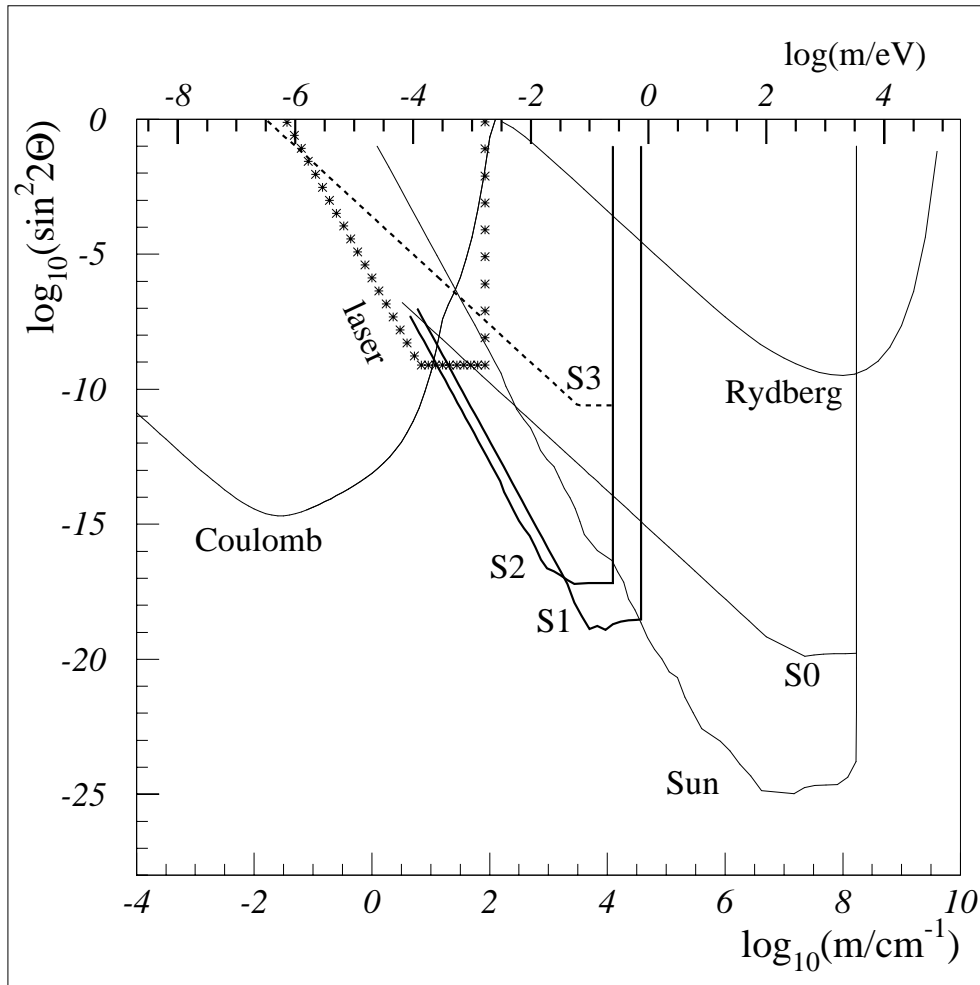


**Figure 1.** Constraints on mixing parameters. Curve marked **Coulomb** stands for a combined result of experiments to test the Coulomb law;  
**Rydberg** : comparing the Rydberg constants for different atomic transitions;  
**laser** : a result of laser experiment;  
**Sun** : solar energy balance.  
 The experiments sensitive to the solar paraphotons :  
**S0** : in the KeV-region, with a proportional chamber(performed);  
**S1** : in the UV-region with a Čerenkov detector (running);  
**S2** : in the visible region with a PMT (proposed);  
**S3** : the same as previous when taking a Sun as a source of photons only.

detect the photons produced by inverse oscillations in the path from this window to the photosensitive element. The details of three experiments are collected in Table 1. We describe here briefly the proposed experiment [17] on the solar telescope.

Experiment	[15]	[16]	[17]
Spectral region	2.8 ... 8.8 KeV	5.5 ... 8.5 eV <sup>2</sup>	2 ... 3 eV
Detector	Proportional chamber	RICH [18]	PMT
Average efficiency	0.4	0.3	0.2
Noise rate, Hz	2	100 <sup>3</sup>	~ 0.1
Sensitive area, cm <sup>2</sup>	19	50,000 <sup>4</sup>	1250
Counting time	~ 1 hour	~ 1 month	~ 3 months
Current state	performed	running	proposed
Curve in Fig. 1	<b>S0</b>	<b>S1</b>	<b>S2/S3</b>

**Table 1.** A summary of the “solar” experiments

The experimental setup with the solar telescope is sketched at Figure 2. The telescope setup could totally be shielded from the light so that the path between the closure and the first optical element (a mirror) serves as an oscillations base. The resulting photons are collected by the slightly modified telescope optics and directed onto the detector. The main element of it is a multi-anode photomultiplier (PMT) with a cooled window. The focussing is made in a way shown at Fig. 2b); in fact, it could be described as looking for a Sun image in paraphotons. With that, one can count signals and backgrounds simultaneously. It eliminates the problem of equalizing the *ON* and *OFF* times for the price of a larger number of readout channels demanding accurate intercalibration. A veto scintillator counter could be installed optionally close to the PMT face in order to cut some of the cosmic background without large distortion of the Sun image.

All three experiments are sensitive also to the paraphotons that appear in solar light *after* it leaves a Sun, so the Sun is taken just as a source of light [19]. But it gives a weaker sensitivity to the mixing parameters (compare the curves **S2** and **S3** for the experiment [17]).

### Conclusions

Described experiments are very complementary over the regions of search and the technics used. The result [14] can not be taken as a firm evidence for existence of the photon regeneration; yet it looks encouraging for the new searches. One can note that the formalism of photon oscillations introduced in [1] may describe exotics that results not only from the parameterization (1). It could be applied also for a photon mixing with another vector particles. The electrodynamics appears to be the most established part of the particle physics and it is a challenging task to search for the limits of its validity.

<sup>2</sup>This detector has also some sensitivity for higher energies (under investigation).

<sup>3</sup>An estimate; much lower values could be reached if the thermal noises only are considered.

<sup>4</sup>An estimate of the effective value (5 m<sup>2</sup> out of total of 25).

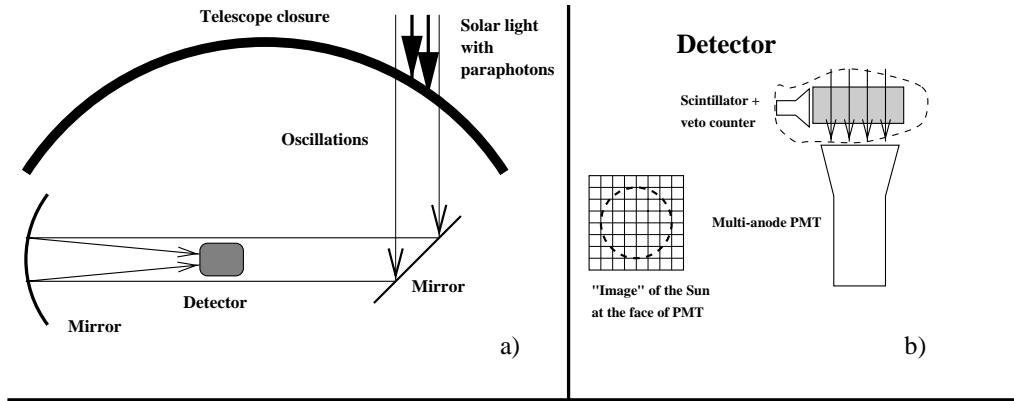


Figure 2. a) A possible layout of experiment, b) detector.

### Acknowledgments

Author is grateful to P. Baillon for the discussions concerning experimental opportunities. The idea of using SAI (Moscow) solar telescope facilities was proposed by O. Goncharenko and V. Somov; E. Guschin helped to finalize a choice of the setup. Critical comments of V. M. Dubovik and S. B. Gerasimov are highly appreciated. Very special thanks come to A. Horzela and E. Kapuscik for creating a warm and stimulating atmosphere at the Workshop.

### References

- [1] L.B.Okun, *Zh. Exp. and Th. Phys.*, **83**(1982) 892 (*Sov. Phys JETP*, **56** (1982) 502).
- [2] I.Yu.Kobzarev and L.B.Okun, *Usp. Fiz. Nauk*, **95**(1968) 131.
- [3] A.S.Goldhaber, M.M.Nieto, *Rev. Mod. Phys.*, **43** (1971) 277.
- [4] L.Davis, jr., A.S.Goldhaber and M.M.Nieto, *Phys. Rev. Lett.*, **35** (1975) 1402.
- [5] V. A. Kostelecky, M. M. Nieto, *Phys. Lett.***B317** (1993) 223; E. Fischbach, H. Kloor, M. Peredo, *Phys. Rev. Lett.***73** (1994) 514.
- [6] V.V.Popov and O.V.Vasil'ev, *Europhys. Lett.*, **15** (1991) 7.
- [7] G.D.Cochran and P.A.Franken, *Bull. Am. Phys. Soc.*, **13** (1968) 1379; D.F.Bartlett, E.A.Phillips and P.E.Goldhagen, *Phys. Rev.*, **D2** (1970) 721.; E.R.Williams, J.E.Faller and H.Hill, *Phys. Rev. Lett.*, **26** (1971) 721.
- [8] R. G. Beausoleil *et.al.*, *Phys. Rev. A*, **35** (1987) 4878.
- [9] S. M. Bilenky, B. Pontecorvo *Phys. Rep.* **41** (1978) 225.



- [10] L. Wolfenstein, *Phys. Rev.*, **D17** (1978) 2369,  
S.P. Mikheev, A. Yu. Smirnov, *Sov. J. Nucl. Phys.* **42** (1986) 913.
- [11] J.N. Bahcall, M.H. Pinsonneault, *Rev. Mod. Phys.*, **67** (1995) 781 ;  
URL: <http://www.sns.ias.edu/~jnb/Html/neutrino.html> .
- [12] J. Christensen-Dalsgaard *et al.*, *Science*, **272** (1996) 1286  
URL: <http://www.obs.aau.dk/~jcd/adipack.n/> .
- [13] N. H. Magee, Jr., J. Abdallah, Jr., R. E. H. Clark, *et al.*, in: *Astronomical Society of the Pacific Conference Series (Astrophysical Applications of Powerful New Databases)*, eds. S. J. Adelman and W. L. Wiese **78** (1995) 51.  
URL: <http://t4.lanl.gov/opacity/tops.html> .
- [14] R. Cameron, G. Cantatore, A. C. Melissinos *et al.*, *Phys. Rev.*, **D47** (1993) 3707.
- [15] D. M. Lazarus, G. C. Smith, R. Cameron *et al.*, *Phys. Rev. Lett.*, **69** (1992) 2333.
- [16] P. Baillon. Search for para-photons with DELPHI RICH. DELPHI Note 96-172 PHYS 661, CERN, Geneva, Switzerland.
- [17] O. Goncharenko, E. Guschin, V. Popov, B. Somov, I. Nikulin, *An experiment to search for the photon regeneration*, Inst. for Nucl. Research (Moscow) and Sternberg Astron. Inst. of Moscow Univ. Letter of Intent, Moscow, 1998.
- [18] P. Abreu *et al.* (DELPHI Collaboration), *Nucl. Instr. and Meth. A*, **378** (1996) 57.
- [19] O. Goncharenko, V. Popov, Preprint LIP-PHYS/93-03, LIP, Lisboa, Portugal.